Study on Hysteretic Bond Mechanisms of Plain Round Bar

Cheng HONG[1], Hideo ARAKI[2]

[1] *Hiroshima University, Japan*
[2] *Hiroshima Institute of Technology, Faculty of Engineering, Japan*
[1]*1-4-1 Kagamiyama Higashi-hiroshimashi, Hiroshima;　d111927@hiroshima-u.ac.jp*
[2]*2-1-1 Miyake Saekiku Hiroshimashi Hiroshima;　h.araki.k4@it-hiroshima.ac.jp*

ABSTRACT

Plain round bars were commonly used as main bars in the design of reinforced concrete (RC) buildings prior to the 1970s. According to previous research investigating the seismic performance of reinforced concrete members constructed with plain round bars, the strength of those members did not reach the calculated flexural strength due to bond slippage of main bars before yielding. It is important, therefore, to investigate the hysteretic bond mechanisms of plain round bars in concrete.

In this research, analytical models were proposed to predict hysteretic bond-slip mechanisms between plain round bar and concrete depending on the results of experiments performed by the authors. In addition, the energy absorption capacity and the equivalent viscous damping factors obtained from the experimental results and analytical models are discussed. As a result of comparisons between the experimental data and the analysis models, good agreements were obtained.

Keywords. plain round bar, epoxy resin injection, analytical models, energy absorption capacity, equivalent viscous damping factor

INTRODUCTION

Many existing RC buildings constructed with plain round bars as the main bars have been judged to have high seismic risk in major earthquakes. In order to evaluate the seismic performance of those buildings, many research projects have been conducted. It has been reported that the maximum strength of those RC members with plain round bars does not reach the calculated flexural strength. The cause of this low capacity is thought to be because bond slip failure occurs before yielding of the main bars. Because the hysteresis loops of axial load deflection curves were presented as slip type due to slip failure, those members possessed very poor energy absorption capacity (Hiroaki TANIGUCHI, 2008). Therefore, bond characteristics between plain round bar and concrete is considered an essential factor affecting the seismic performance of existing RC buildings. However, the influence of the above bond characteristic are not considered in the present seismic evaluation for existing RC buildings.

Table 1. List of Specimens Subject to Monotonic Loading

Series of Specimens	Number of Specimens	Steel	Direction of Casting	Location of Steel
HR13-9	5	13φ	Horizontal	Centre
VR13-9	3		Vertical	
HR13-9-B	3		Horizontal	Bottom
HR19-9	5	19φ	Horizontal	Centre
VR19-9	3		Vertical	
HR19-9-B	3		Horizontal	Bottom

Table 2. List of Specimens Subject to Cyclic Loading

Series of Specimens	Number of Specimens	Steel	Direction of Casting	Location of Steel
HR13-9-R	3	13φ	Horizontal	Centre
HR13-9-R	3	19φ		
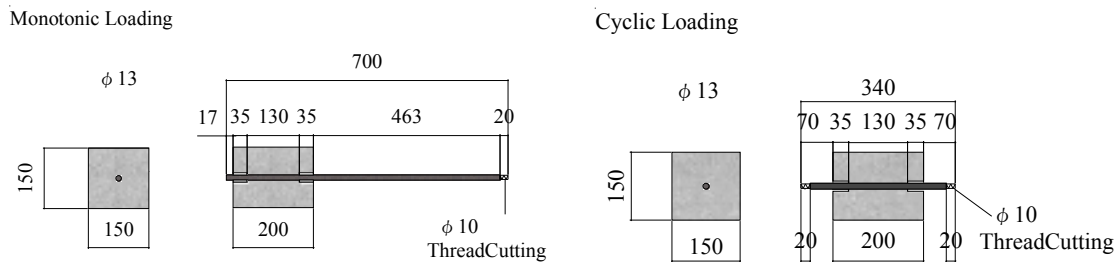
Figure 1. Details of Specimens

To resist sever earthquakes in Japan, retrofitting and strengthening techniques for existing structures have been in development since 1970. One of the most effective techniques has been epoxy resin injection, which improves the bond strength between the main steel bars and the concrete. The seismic of damaged columns repaired with epoxy resin injection has been laboratory tested at Hiroshima University, and it was reported that the flexural strength and ductility of those retrofitted columns increased (Hideo ARAKI, 2012). One of the authors also investigated bond strength through pull-out tests using concrete prisms with plain round bars injected with epoxy resin. A significant improvement in bond strength was observed in those tests (Hideo ARAKI, 2010).

In this paper, an analytical model of bond hysteresis for plain round bar retrofitted with epoxy resin is proposed in order to investigate the seismic performance of the RC members in existing buildings. Following this, the validity of the proposed bond-slip model is confirmed in comparison with the observed bond-slip hysteresis. The levels of energy absorption capacity and the equivalent viscous damping factors derived from the experimental data and analytical model are also discussed in this paper.

EXPERIMENTAL PROCEDURE
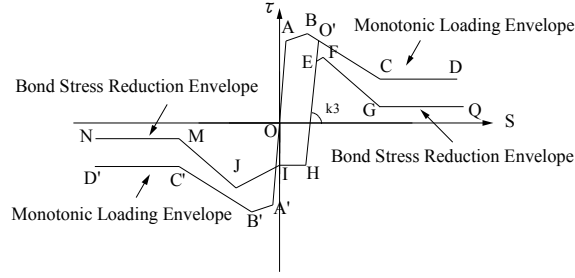
Figure 2. Fundamental Bond-Slip model

Test specimens and material. Each of the specimens used for the pull-out tests was a concrete prism with a plain round bar embedded axially. Each bar was arranged horizontally in the concrete prism corresponding to bars in horizontal members of the beam. A series of pull-out specimens subjected to monotonic loading is listed in Table 1, those subjected to cyclic loading are listed in Table 2, and details of the specimens are illustrated in Figure 1. In all specimens the specified concrete strength was 9MPa. The considered variables were the diameters of the bar (13φ, 19φ), the direction of the concrete casting, and the location of the bars. All of the mechanical characteristics of concrete and steel were the same as for previous tests (Cheng HONG,2012).

Testing procedure and epoxy resin injection. The testing setup and procedures were essentially the same as the previous pullout test, and the epoxy resin injection method was low viscous epoxy resin of 100~ 200 mPa.s which was injected at a very low pressure of 0.06 N/mm². Both the testing procedures and epoxy resin injection method can refer to in the pervious study (Cheng HONG,2012).

EXPERIMENTAL RESULTS

Bond-Slip Model. According to the proposed bond-slip model without retrofitting in the previous test (Cheng HONG, 2012), the new analytical approach to predicting the hysteresis bond-slip relationship of the specimens with retrofitting was also divided into two parts: envelopes for monotonic loading and hysteresis loops for cyclic loading as follows:

Envelope for Monotonic Envelope. Figure 2 shows the fundamental analytical bond-slip model of retrofitted specimens. Each point in the monotonic loading envelope was obtained from regression analysis using the experimental data of the monotonic pull-out specimens in Table 1. In the figure, points A C D were determined using point B (τ_{Max}, S_{Max}) as the maximum bond strength. τ_{Max} was the average maximum bond strength of each series specimens in this paper. The experimental value of S_{Max} ranged from 0 to 0.448mm, therefore S_{Max} was proposed to be 0.2mm here.
The envelope composed of the ascending zone shows as route O-A and A-B, the descending zone as route B-C, and the stability zone as route C-D. The bond strength of envelopes in the ascending zone is presented by Eq.(1)

$$S \leq S_A \qquad \tau = K_1 \cdot S$$
$$S_A < S \leq S_B \quad \tau = K_2 \cdot (S - S_A) + \tau_A \tag{1}$$
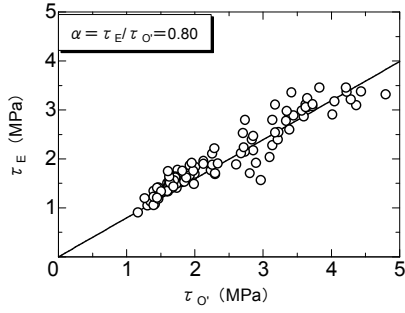
Figure 3. Regression analysis of parameter α   **Figure 4.** Load reversed at O-A
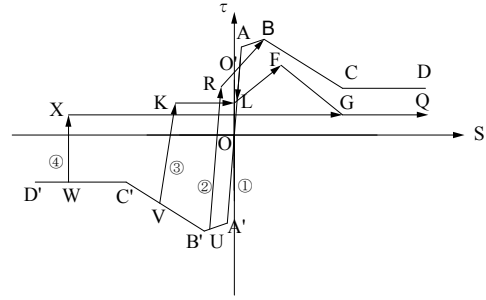
Parameters $K_1=\tau_A/S_A=2.375$ K_B N/mm^3 and $K_2=(\tau_B-\tau_A)/(S_B-S_A)=0.083$ K_B N/mm^3 were obtained from the experimental results of the ascending zone. $K_B=\tau_B/S_B$ is the equivalent stiffness at point B. Point A~D are presented as Eq.(2).

$$A(\tau_A,S_A)=(0.95\tau_{Max},0.40S_{Max}), \; B(\tau_{Max},S_{Max})=(\tau_{Max},0.2mm)$$
$$C(\tau_C,S_C)=(0.50\tau_{Max},5mm), \; D(\tau_D,S_D)=(0.50\tau_{Max},S>5mm) \tag{2}$$

Envelopes for Cyclic Loading. The proposed envelope under reversal load is also shown in Figure 2 based on the experimental data of the specimens shown in Table 2. After cyclic loading, when the load was reversed in the path O′-H the strength reached point E. Point E is represented by Eq. (3) using the coordinate of point O′.

$$E(\tau_E,S_E)=(\alpha\tau_{O'},S_{O'}-(1-\alpha)\tau_{O'}/K_3) \tag{3}$$

α in Eq.(3) is a reduction factor ($\alpha=\tau_E/\tau_{O'}$) to the bond strength of the previous loading where α is assumed to be 0.80 can refer to Figure 3. $K_3=|\tau_{O'}-\tau_H|/|S_{O'}-\tau_H|=54.3$N/mm^3 is obtained from experimental data shown in Table 2. Bond strength was assumed to decrease from point F in the case that the load increased from point E. Point F is represented by Eq. (4) using the coordinate of point O′.

$$F(\tau_F,S_F)=(0.89\tau_{O'},1.13S_{O'}) \tag{4}$$

The bond strength decreased to point G through path F-G. Point G was represented by Eq. (5) in the previous reference.

$$G(\tau_G,S_G)=(0.22\tau_{Max},5mm) \tag{5}$$

The envelope J-M-N on the negative side was symmetrical to F-G-Q.

Hysteresis Rules of Cyclic Loading. Morita (1974) proposed the hysteresis characteristics of deformed bars. Referring to the proposed hysteresis bond-slip characteristics, the analytical bond-slip model for plain round bars when unloaded from ascending zone (O-A-B) can be determined as the following:
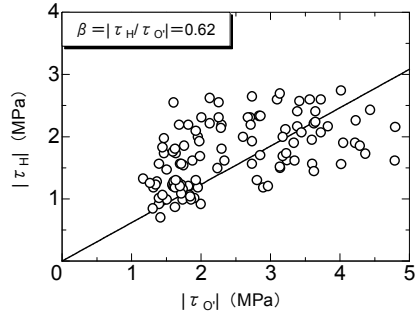
Figure 5. Regression analysis of parameter β   **Figure 6.** Load reversed at A-B
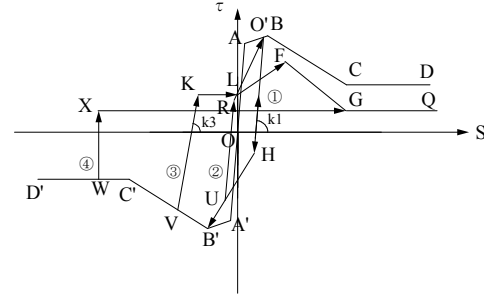
When Unloaded from Ascending Zone (O-A). When the load was reversed from point O′ at path O-A, the load-deflection relationship is elastic, and hysteresis rules are shown in Figure 4.

The path is: O′-A′-B′-C′-D′

Assuming that the load was reversed at point O″, the following bond-slip curve can be divided into four cases, as follows:

(1) $S_{A'} \leqq S_{O''} < S_A$

When the load was in path A′-O-A, load-deflection relationship is elastic.

(2) $S_{B'} \leqq S_{O''} < S_{A'}$

When the load was reversed from point U at path B′-A′, the bond-slip path was U-R-B-C-D. Point R is represented by Eq.(6) using the coordinate of point U.

$$R(\tau_R, S_R) = \left(-\beta\tau_U, S_U - (1+\beta)\tau_U / K_1\right) \tag{6}$$

where $\beta = |\tau_H/\tau_{O'}|$ is a parameter defined as the reduction of 0.62 can refer to Figure 5.

(3) $S_{C'} \leqq S_{O''} < S_{B'}$

When the load was reversed from point V at path B′-C′, the stiffness is the same as stiffness K_1 up to point K. The bond strength of point K is consist until slip deflection approaches to the previous point L. The bond-slip path in this case was V-K-L-F-G-Q, and point K and F are shown in Eq.(7) and Eq.(8) using the coordinate of point V.

$$K(\tau_K, S_K) = \left(-\beta\tau_V, S_V - (1+\beta)\tau_V / K_3\right) \tag{7}$$

$$F(\tau_F, S_F) = \left(0.89\tau_V, 1.13S_V\right) \tag{8}$$

(4) $S_{O''} < S_{C'}$

When the load was reversed from a point between C′ and D′ the bond strength was assumed constant until the ultimate slip deflection.The bond-slip path was W-X-G-Q, and the point X is shown in Eq. (9) using the coordinate of point W.

$$X(\tau_X, S_X) = \left(0.22\tau_{Max}, S_W\right) \tag{9}$$

When Unloaded Rule from Ascending Zone (A-B). Figure 6 shows the analytical model when the load was reversed from point O′ in the path A-B. The stiffness was assumed
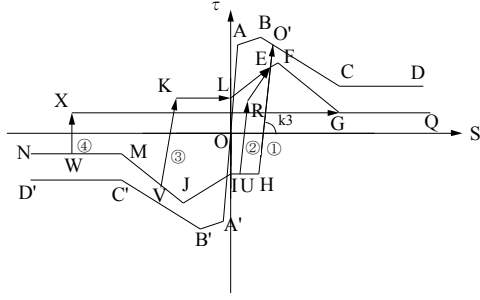
Figure 7. Load reversed at B-C　　　　　**Figure 8.** Load reverse at C-D
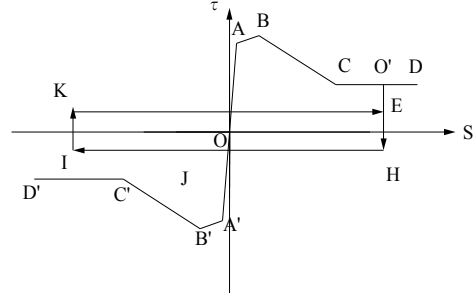
to be K_1 to point H. After point H the strength return to point B′. On the negative side, the bond-slip envelope followed the monotonic loading envelope.

The path is: O′-H-B′-C′-D′

Assuming that the load was reversed at point O″, the following bond-slip curve can also be divided into four cases, as follows:

(1) $S_{O''} \geqq S_H$

The bond-slip path followed a linear unloading line with the stiffness K_1 and reached the monotonic loading envelope on the positive side.

(2) $S_{B'} \leqq S_{O''} < S_H$

When the load was reversed at point U in path B′-H, the bond-slip path was U-R-B-C-D. Point R is represented by Eq. (10) using the coordinate of the previous point U.

$$R(\tau_R, S_R) = \left(-\beta \tau_U, S_U - (1+\beta)\tau_U / K_1\right) \tag{10}$$

(3) $S_{C'} \leqq S_{O''} < S_B$

When the load was reversed at point V in path B′- C′ the bond-slip path was the same as the previously mentioned case (3).

(4) $S_{O''} < S_{C'}$

When the load was reversed at a point in the constant strength zone C′-D′, the bond-slip relationship was the same as the previously mentioned case (4).

Unloaded at Descending Zone (B-C). Figure 7 shows the analytical model when the load was reversed in path B-C. When the load was reversed at point O′, bond strength decreased with stiffness K_3 and reached point H on the opposite side. Point H is represented by Eq. (11) using the coordinate of point O′.

$$H(\tau_H, S_H) = \left(-\beta \tau_{O'}, S_{O'} - (1+\beta)\tau_{O'} / K_3\right) \tag{11}$$

Slip deflection reached point I while bond strength was constant. When the slip deflection reached the negative area, the bond strength increased up to point J. After point J the strength reached point M. Finally, bond strength became constant. When the load was reversed in path H-I-J-M-N, the following bond-slip curve could also be divided into four parts:

(1) $S_H \leqq S_{O''} < S_{O'}$

When the load was reversed from a point at path O′-H, the bond-slip path followed a linear unloading path with stiffness K_3 and reached the monotonic loading envelope on the positive side.
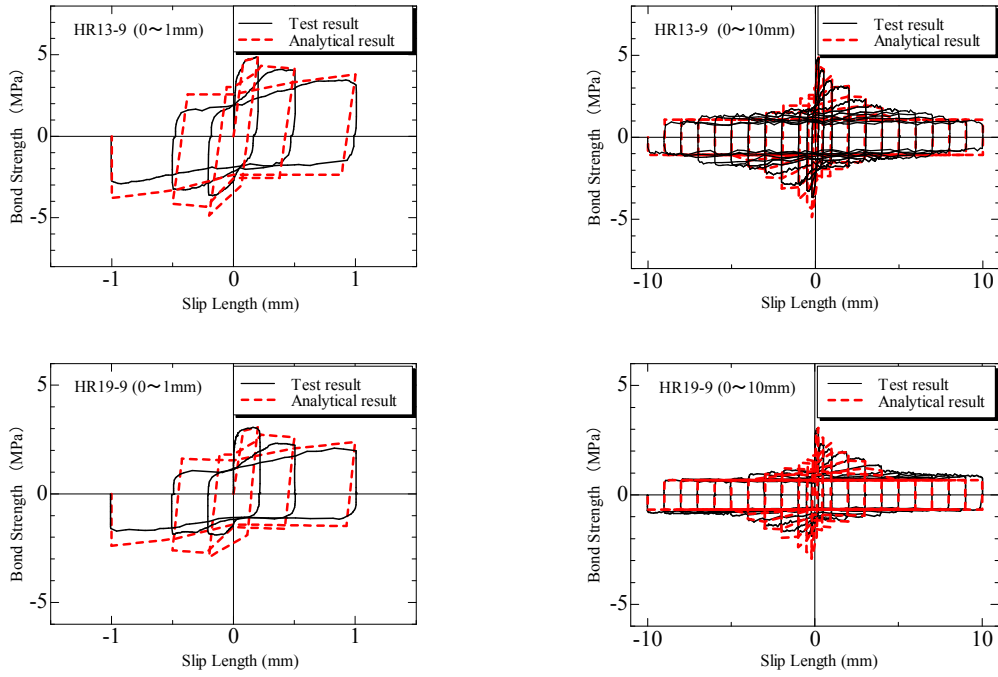
Figure 9. Comparisons between test results and analytical model

(2) $0 \leqq S_{O''} < S_H$

When the load was reversed from point U at path I-H, the bond-slip path was U-R-E-F-G-Q. Point R is shown in Eq. (12) using the coordinate of point U.

$$R(\tau_R, S_R) = \left(-\beta\tau_U, S_U - (1+\beta)\tau_U / K_3 \right) \tag{12}$$

(3) $S_M \leqq S_{O''} < 0$

When the load was reversed from point V at path M-I, the bond-slip path was V-K-L-E-F-G-Q. Point K was shown in Eq. (13) using the coordinate of point V.

$$K(\tau_K, S_K) = \left(-\beta\tau_V, S_V - (1+\beta)\tau_V / K_3 \right) \tag{13}$$

However, if $\tau_K = -\beta\tau_V \leq 0.22\tau_{Max}$, value of τ_K was assumed to be $0.07\tau_B$.

(4) $S_{O''} < S_M$

When the load was reversed in the large slip length area, the bond-slip relationship was the same as the previously mentioned case (4).

Unloaded at the stability zone (C-D). Figure 8 shows the analytical model when the load was reversed in path C-D or G-Q. The bond strength decreased without change of slip deflection and reached the constant strength $\tau = -0.22\tau_{Max}$.

Comparisons with Test Results and Proposed Model. Figure 9 shows comparisons between the test results of 13ϕ and 19ϕ specimens and the proposed bond-slip model, with a small slip deflection (0~1mm) and large slip deflection (0~10mm). The bond-slip model provided approximate agreement with the test results. However, some differences could be
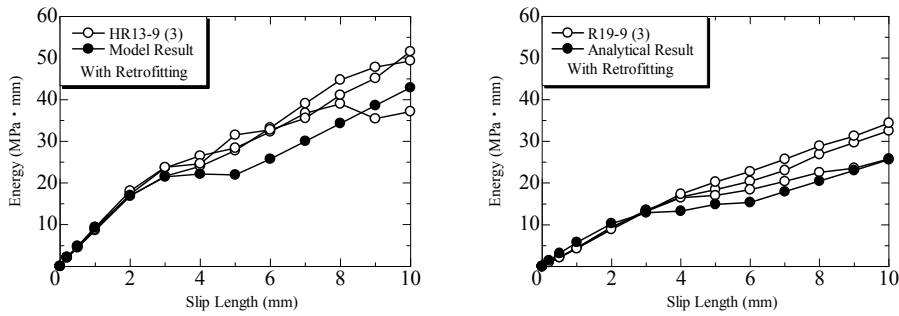
Figure 10. Energy absorption capacity versus slip length
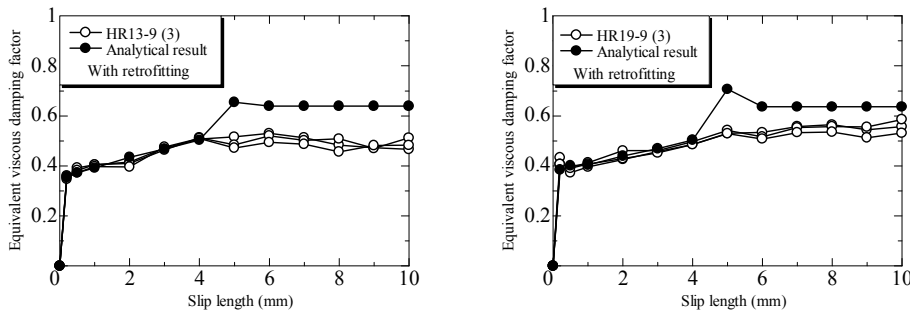
Figure 11. Equivalent viscous damping factor versus slip length

found due to parameters α and β, which were influenced by the number of loading cycles.

DISCUSSION ON SEISMIC PERFORMANCE

Figure 10 and Figure 11 show energy absorption capacity, and equivalent viscous damping factor versus slip length, respectively. The analytical results are also inserted into the figure. The analytical model results depended on the average maximum bond strength of each series. According to the previous experimental results, the average maximum bond strength of specimens with retrofitting for φ13 was 4.88MPa, and for φ13 was 2.91MPa.

As shown in Figure 10, the calculated energy absorption capacity of each cycle for φ13 and φ19 is scattered in the range of 2.13 to 51.23 MPa・mm and 1.11 to 30.91 MPa・mm, respectively. The energy absorption capacity of the specimens with retrofitting for 13φ bar was significantly higher than that of 19φ.

As shown in Figure 11, the equivalent viscous damping factor in each cycle was also nearly the same. The value was in the range of about 40% to 50%. The analytical results provided good agreement with the experimental results.

CONCLUSIONS

Based on all of the analytical investigations, the following conclusions can be made:
(1) The analytical models of bond characteristics were proposed based on the test results.
(2) The proposed models provided good agreement with the experimental results.
(3) The energy absorption capacity for 13φ bar was significantly higher than that of 19φ.
(4) The energy absorption capacity and equivalent viscous damping factor of the specimens retrofitted by epoxy resin injection showed good performance.

ACKNOWLEDGEMENT

REFERENCES

Cheng, HONG, Hideo, ARAKI; Bond-Slip Relationship between Low strength Concrete and Plain Round Bar under Reversal Loadings, Proceedings of 15th World Conference on Earthquake Engineering, Lisbon, PORTUGAL, (2012)

Hiroaki, TANIGUCHI, Akira, YASOJIMA, Hideo, ARAKI; Seismic performance of Reinforced Concrete Beams with Low Strength Concrete, Proceeding of 14th Word Conference on Earthquake Engineering, Beijing, China, Paper ID-05-03-0034(2008)

Hideo, ARAKI. Seiya, IZAKI; Seismic Performance of Damaged Low Strength Concrete Column Repaired by Epoxy Resin Injection, Journal of Architectural Institute of Japan, 18(38):181-186, (2012)

Hideo, ARAKI. Junichi, KAGAWA; Bond Strength of Plain Round Bars Repaired by Epoxy Resin Injection, The 34th IABSE Symposium, Italy, Venice,(2010)

Morita S, Kaku T, Local bond stress-slip under repeated loading. In: Theme IV, Rilem Symposium, Prague; 1974